

Investigation of Wear and Adhesion Behaviors of Borided Steels

Rıza Kara¹ · Fatih Çolak¹ · Yusuf Kayali²

Received: 22 April 2015 / Accepted: 20 August 2015 / Published online: 21 November 2015
© The Indian Institute of Metals - IIM 2015

Abstract In this study, AISI P20, H13 and D2 steels were pack borided at 900 and 950 °C for retention times of 2, 4 and 6 h. The boride layer thickness values changed depending on the chemical composition of the steels. The hardness of borides that formed on the surface of AISI P20, AISI H13 and AISI D2 steels were 1897 HV(50 g), 1989 HV(50 g) and 1916 HV(50 g), respectively. On the other hand, the Vickers hardness values of the untreated steels were 532 HV(50 g), 485 HV(50 g) and 408 HV(50 g), respectively. The adhesion properties of the boride layer were analyzed by performing the Daimler–Benz Rockwell-C adhesion method. According to the adhesion and wear test results, the adhesion and wear resistance of the boride layer decreased with the increase in the boriding temperature and time.

Keywords AISI P20 · AISI H13 · AISI D2 · Boriding · Rockwell-C indentation · Adhesion · Wear resistance

1 Introduction

Boriding is a thermochemical surface hardening process which strengthens the surface of a material with the diffusion of boron atoms onto the metal surface. The borides

formed as a result of the boriding process improves the tribological behavior of the steel substrate [1]. With the boriding method, which has been practiced since the beginning of the twentieth century, it is now possible to produce high strength and wear-resistant materials which have low coefficient of friction. With the boriding process, which is a thermochemical surface hardening method, boron atoms diffuse into the metal surface thermochemically and form a hard boride layer. Industrial boriding can successfully be applied to steels, cast iron, nickel, cobalt, titanium, molybdenum-based alloys and numerous ferrous and non-ferrous metals such as cermet carbides at temperatures of 700–1000 °C for 1–10 h in a solid, liquid, gas, or plasma medium [2]. The pack boriding method, which is similar to the carburizing process, is widely preferred. Compared to other methods, pack boriding has advantages due to the fact that it is cost-effective and easily-applicable [3, 4].

The most important feature of the boriding process is that the obtained boride layer has very high hardness (1400–3000 HV), wear resistance, fusion temperature and coefficient of friction [5]. The boride layer is also capable of maintaining its hardness at higher temperatures (550–600 °C). In addition, it improves the corrosion and erosion resistance of ferrous materials against non-oxidising dilute acids [6]. Since boride layers are brittle, they are not preferred in applications subjected to impact loads [5].

AISI P20 steels are known as die steels. The surfaces of these steels are expected to be hard [7]. AISI H13 hot work tool steel is widely used in metal injection moulds, extrusion molds of light metals, forging dies and plastic injection molds [6]. AISI D2 cold work tool steel has a wide application scale because it has high hardenability and low distortion after quenching. It is possible to improve the surface hardness and wear behaviors of cold work tool

✉ Rıza Kara
riza.kara@usak.edu.tr

¹ Department of Mechanical and Metal Technologies,
Vocational School of Technical Sciences, Uşak University,
64000 Usak, Turkey

² Department of Metallurgical and Materials Engineering,
Technology Faculty, Afyon Kocatepe University, 03200
Afyon, Turkey

steels through surface operations [8]. Taking into account the high surface hardness, low friction, high wear and corrosion resistance provided by boriding, AISI P20, AISI H13 and AISI D2 steels were borided with the pack boriding method. The optical microstructure, the layer thickness values, the resulting phases and the surface hardness values of the boride layer were determined. Wear and adhesion behaviors of the borided steels were investigated.

2 Experimental Procedures

2.1 Boriding and Characterization

Substrate materials used in this study were AISI P20 steel, AISI H13 steel and AISI D2 steel. The chemical compositions of test materials are given in Table 1. The test samples dimensions were $\text{Ø}17 \times 6$ mm. Before boriding treatment, specimens were ground up to 1200 mesh emery paper and then polished using 1 micron diamond pastes. Boriding heat treatment was carried out in the solid medium consisting of Ekabor-II powder

mixture in an electrical resistant furnace under atmospheric pressure at 850, 900 and 950 °C temperatures for retention times of 2, 4, and 6 h followed by air cooling. All test samples to be boronized were packed in the powder mix and sealed in a stainless steel container. The boxes were firmly closed in order to make them air proof. At the end of boronizing, the boxes were cooled to room temperature and then the test samples were removed from the pack.

The microstructures of polished and etched cross-sections of the samples were observed by an optical microscope (Olympus BX-60) and scanning electron microscopy (SEM) (Leo 1430VP). The presence of borides formed in the coating layer was confirmed by means of X-ray diffraction (Shimadzu XRD-6000) using $\text{CuK}\alpha$ ($\lambda = 1.5406 \text{ \AA}$) radiation. The thicknesses of borides were measured by means of a digital thickness measuring instrument attached to an optical microscope (Olympus BX60). Thickness values given in the results section are averages of at least 10 measurements. The hardness of the boride layers and substrates was measured on the cross-sections using a Shimadzu HMV-2 Vickers indenter with a 50 g load.

Table 1 The chemical composition of test materials (wt%)

Steel	C	Cr	Ni	Si	Mn	Mo	V	P	S
AISI P20	0.37	1.16	1.12	0.29	1.42	0.17	...	0.011	0.008
AISI H13	0.37	5.20	...	0.82	0.32	1.20	1.01
AISI D2	1.48	11.91	...	0.96	0.45	0.98	0.76

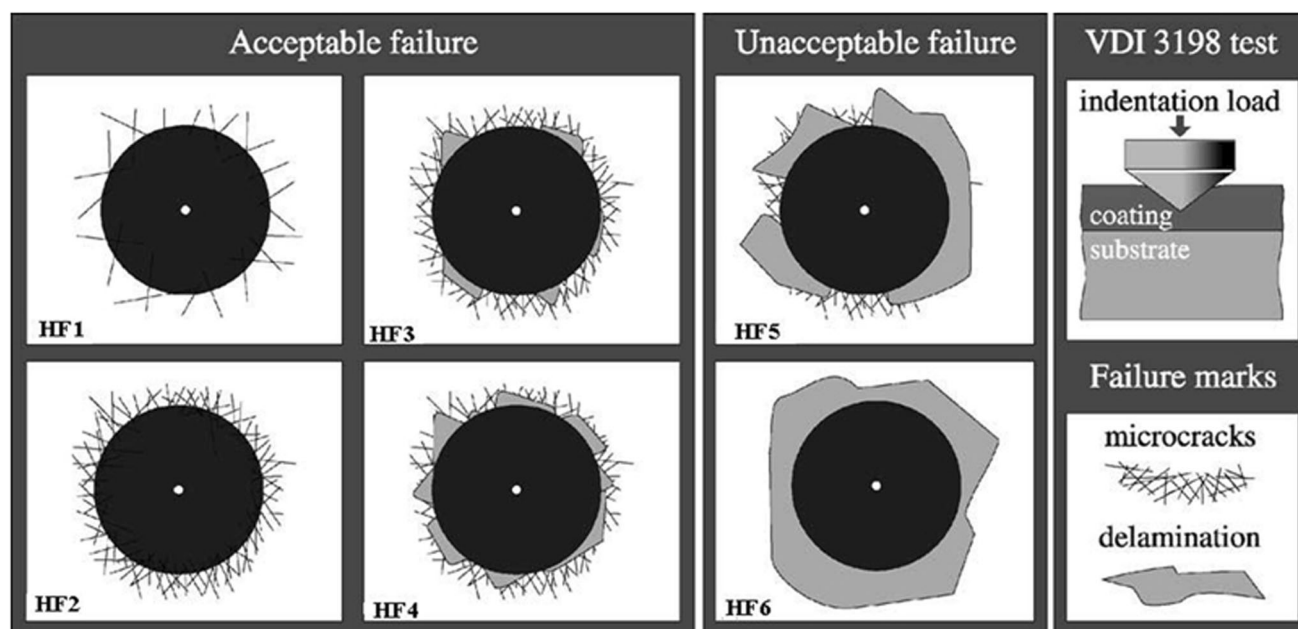


Fig. 1 The principle of the VDI 3198 indentation test

2.2 Adhesion and Wear Tests

The Daimler–Benz Rockwell-C adhesion test was used to assess the adhesion of the boride layers. The well-known HRC indentation test is prescribed by the VDI 3198 norm, as a destructive quality test for coated compounds [6, 9–11]. Figure 1 are four acceptable and two unacceptable damages on these maps. In general, adhesion strength is qualified as sufficient for Fig. 1(HF1–HF4) while it is insufficient for Fig. 1(HF5–HF6) [9, 11].

The principle of this method is represented in right most part of Fig. 1 [9]. A load of 1471 N was applied to cause coating damage adjacent to the boundary of the indentation [12]. Three indentations were conducted for each specimen. Scanning electron microscopy was employed to evaluate the test.

Wear tests of borided steels were carried out with a CSM Instruments Tribometer ball-on-disk tester, using the an 8-mm-diameter WC–Co ball as the pin. The friction force was monitored continuously by means of a force transducer. Unlubricated wear tests were performed at a constant speed (0.3 m/s), with a load of 10 N for 500 m sliding distance at room temperature (25 °C). Before and after each wear test, each sample and abrasion element was cleaned with alcohol.

Wear rates of samples were obtained using the following equation. Thickness of wear track was measured using optical microscopy. Worn surfaces were investigated by scanning electron microscopy.

$$W = \frac{2\pi(R + \frac{L}{2})^2 \frac{r^2}{2} (\theta - \sin \theta)}{\text{Sliding Distance}}$$

where; W is the wear rate (mm^3/Nm), L is the sliding distance (m), L, R is the wear track thickness (mm), R, r is the radius of the wear scar (mm), r, radius of ball (mm) and $\theta = 2 \arcsine(L/2r)$ (radian).

3 Results and Discussion

3.1 Characterization of Boride Coatings

It can be seen in Fig. 2 that the boride layer formed, depending on the chemical composition of the steel has an acicular (saw-tooth) and a flat structure. It is determined that the coating matrix interfacial morphology of AISI P20 steel exhibits an acicular structure (Fig. 2a) [7]. It is also observed that the boride coating, the coating-matrix interface and matrix are clearly separated from each other and that the boride coating has a uniform thickness in all samples. AISI H13 steels in Fig. 2b shows three distinct regions. They are (1) boride layer including borides, (2)

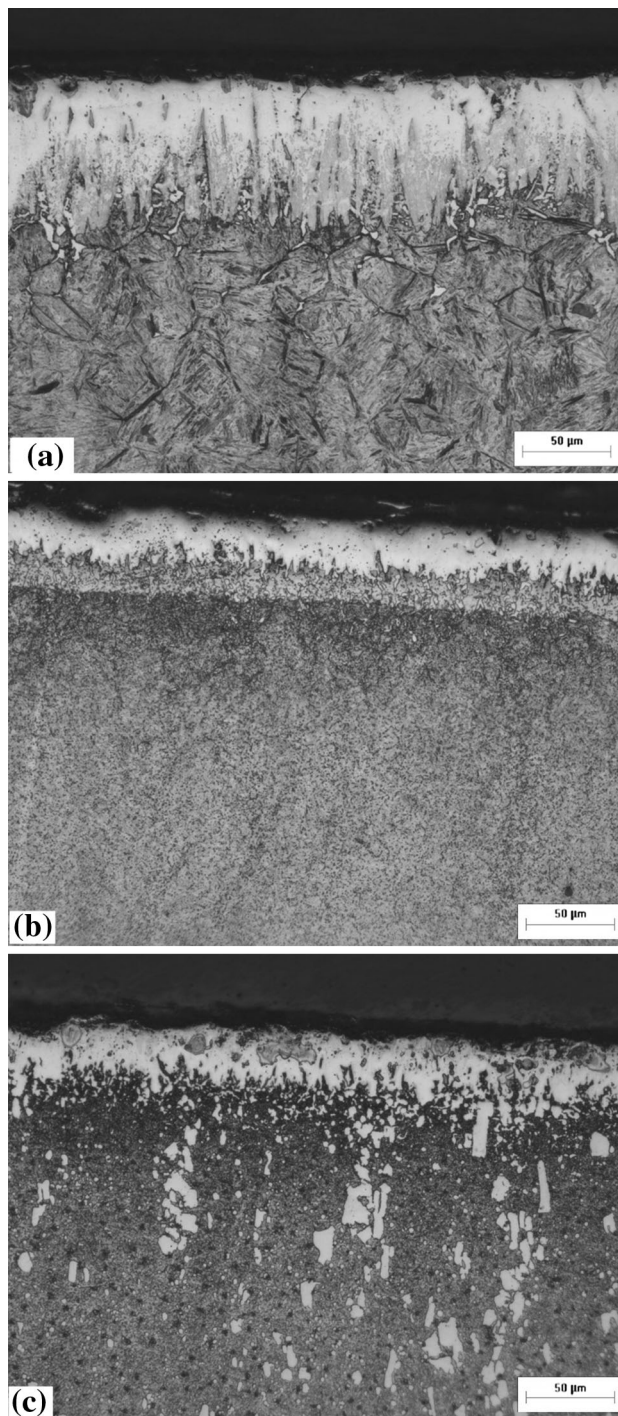


Fig. 2 Optical cross-sectional views of borided **a** AISI P20, **b** AISI H13 and **c** AISI D2 steels at 900 °C for 6 h

transition zone relatively softer than the substrate, (3) matrix that is not affected by boron.

A morphological examination of the boride layer formed on the surfaces of AISI H13 and AISI D2 steels reveals that the coating has a uniform columnar structure (Fig. 2b–c). However, the columnar morphology of the AISI D2 and

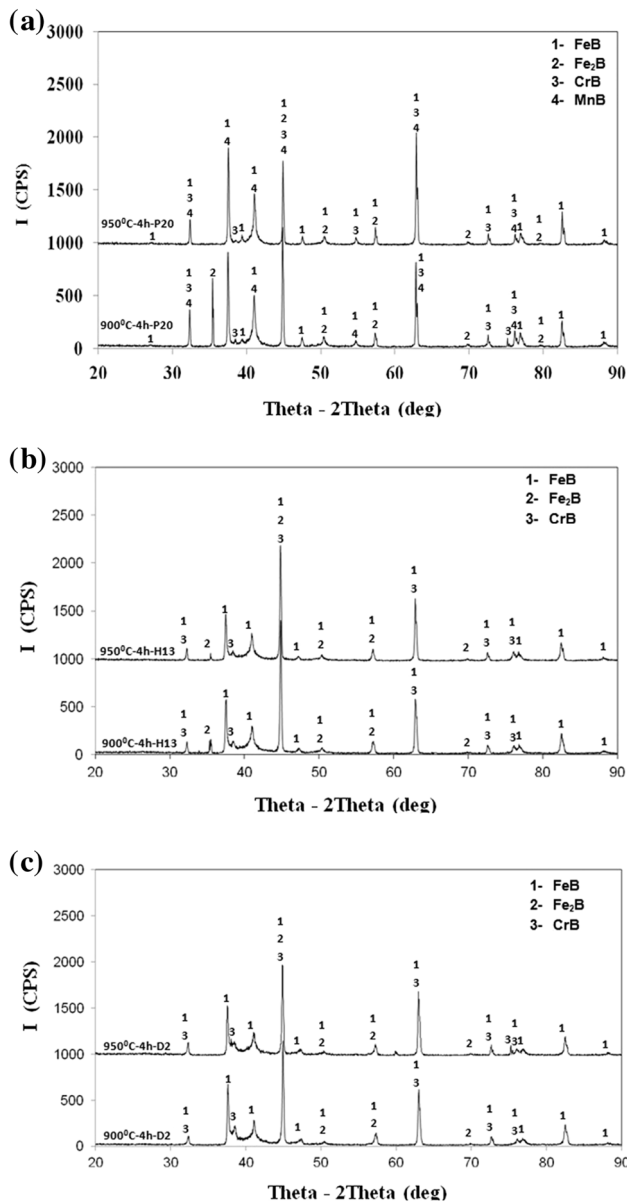


Fig. 3 X-ray diffraction patterns of borided **a** AISI P20, **b** AISI H13 and **c** AISI D2 steels at 900 and 950 °C for 4 h

AISI H13 steels are flatter compared to AISI P20 steels. The boride coating-matrix interface changes from a columnar structure to a flat structure increasing with the amount of Cr in steels. This is because, the alloying elements causes a flat structure of the interface by forming of alloy borides in the boride coating [6, 13–16].

The atomic number of chromium is lower than that of the iron, therefore, the chromium dissolves more in the boride layer ((Fe, Cr)B and (Fe, Cr)₂B) than the substrate and diffuses to the surface. The Chromium affects both the morphology and the layer thickness of the boride layer [5]. As can be seen in Fig. 2, the borides formed have a relatively complex and flat character.

3.2 X-Ray Diffraction Analysis

XRD patterns show that the boride coating consists of MB and M₂B (M = Metal; Fe, Cr) types of borides. XRD analysis of the steels indicate that FeB, Fe₂B, CrB and MnB phases are formed on the boride coating, depending on the chemical composition of the steel. It is observed that FeB, CrB and MnB phases are increases with an increase in the boriding temperature (Fig. 3).

3.3 Thickness of Boride Layer and Hardness

As a result of the boriding process, it was determined that the boride layer thickness values increased depending on the processing time and temperature and that the coating thickness depended on the chemical composition of the steel [6, 17, 18]. The boride layer thickness values of AISI P20, AISI H13 and AISI D2 ranged from 44 to 143 μm, from 20.8 to 85 μm and from 13.3 to 68 μm respectively. The dependence of the boride layer thickness values on the boriding time and temperature are in given Table 2. The thickness of the boride layer formed on the surface of AISI D2 steel was lower than that of AISI P20 and AISI H13 steels. This might be due to the amount of alloying

Table 2 The thickness and microhardness of boride layers on the borided AISI P20, H13 and D2 steels at 900 and 950 °C

Substrate	Boriding temperature (°C)							
	Boriding time (h)							
	900			950			900	950
Layer thickness (μm)						Microhardness (HV _{0.05})		
AISI P20	44 ± 5	74 ± 2	82 ± 3	73 ± 6	111 ± 5	151 ± 3	1797 ± 18	1897 ± 35
AISI H13	21 ± 3	38 ± 7	58 ± 5	40 ± 3	64 ± 8	85 ± 7	1845 ± 24	1989 ± 15
AISI D2	13 ± 3	29 ± 5	35 ± 2	31 ± 4	44 ± 6	67 ± 4	1801 ± 20	1916 ± 55

elements (especially Cr) in AISI D2 steel was greater than that in other steels [6].

Micro-hardness measurements of the boride layer were carried out for each point located at same distance from the surface by means of a Vickers indenter using a load of 50 g. The hardness measurements were performed by taking the average values of at least 7 different measurements and standard deviations. The surface hardness values of AISI P20, AISI H13 and AISI D2 steels increased about fourfold–fivefold during the boriding process. The increase in the hardness values depended on the boriding time and

temperature [6]. Figure 4 illustrates the distribution of hardness values of the three steels from the surface towards the interior. High hardness values were obtained along the boride layer followed by a sudden drop at the matrix. While the hardness values of unborided AISI P20, AISI H13 and AISI D2 steels varied between 408 and 532 HV(50 g), the surface hardness values of the steels after boriding ranged from 932 to 1989 HV(50 g) depending on temperature and time.

3.4 Daimler–Benz Rockwell-C Adhesion Test

Figure 5 shows the Rockwell-C indentation SEM tracks of the steels borided at 900 °C for 2 h. The track seen in Fig. 5a shows that microcracks are formed as in Fig. 1(HF1) of the map developed by Daimler–Benz and that the adhesion of the coating is very good. Hence, it is an acceptable coating. Both Fig. 5b as well as Fig. 1(HF4) show microcracks and delaminations were observed in Fig. 5b as well as in Fig. 1(HF4). This is also an acceptable coating according to the map. Many microcracks are seen in Fig. 5c as well as in Fig. 1(HF2). This indicates that the boriding of AISI D2 steel is an acceptable coating according to the map.

The track in Fig. 6a indicates the formation of microcracks and that the adhesion of the coating is as good as in Fig. 1(HF2) of the map. According to the map, this is also an acceptable coating. Figure 6b–c as well as Fig. 1(HF5) shows both microcracks and delimitations. But this is an unacceptable coating according to the map [11].

Figure 7 illustrates the Rockwell C indentation SEM tracks of AISI H13 steel borided at 900 °C for 2, 4 and 6 h. The microcracks and delamination are observed to increase with an increase in the boriding time. However, this increase in the delimitations is not too high to consider the coating unacceptable, which means that according to the Daimler–Benz in the map, it is an acceptable coating. The adhesion quality of the boride coatings on AISI H13 and AISI D2 steels obtained from the boriding process at 950 °C for 4 and 6 h are insufficient according to the maps. Adhesion strength quality (HF1–HF6) of steels borided at 900 and 950 °C for 2, 4 and 6 h are given in Table 3. It is clear from Table 3 that adhesion quality of borided steels decreases with the increase in boriding temperature except for AISI P20 steel. As can be seen in Figs. 7 and 8, the adhesion quality of the boride layers of all the steels decreases with an increase in the boriding time and temperature. These results are consistent with the literature [6, 19, 20].

3.5 Wear Behaviors

Wear rates obtained from the worn out areas are given in Fig. 9. While the wear rates of the unborided samples

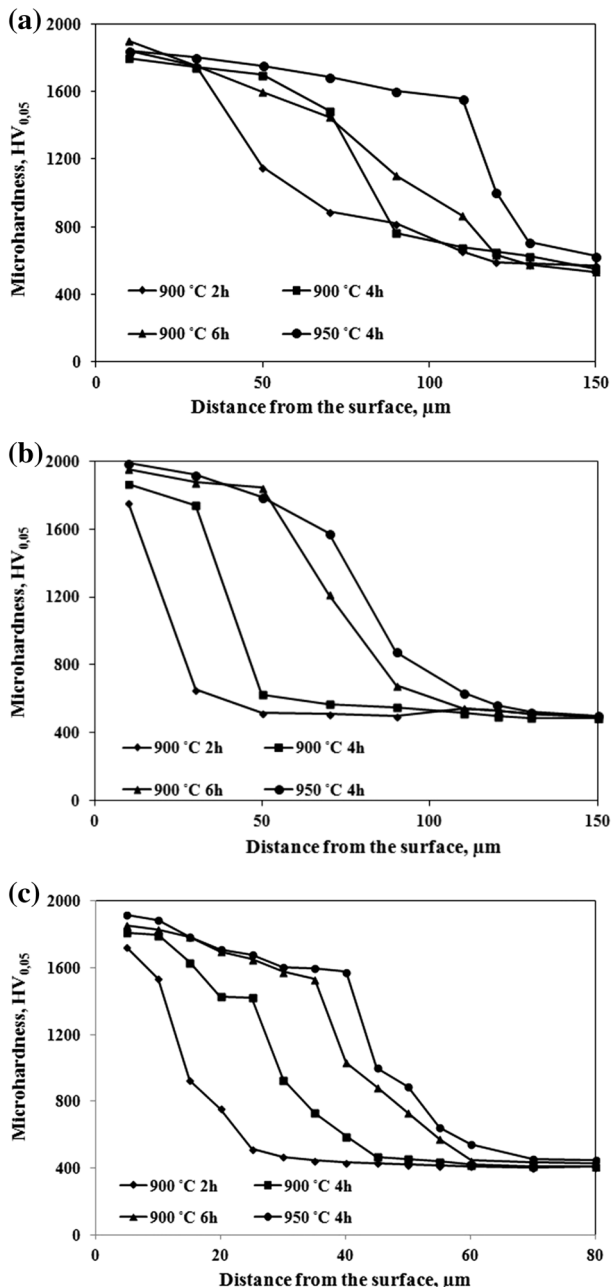


Fig. 4 The variation of micro-hardness of borided a AISI P20, b AISI H13 and c AISI D2 steels from surface to matrix

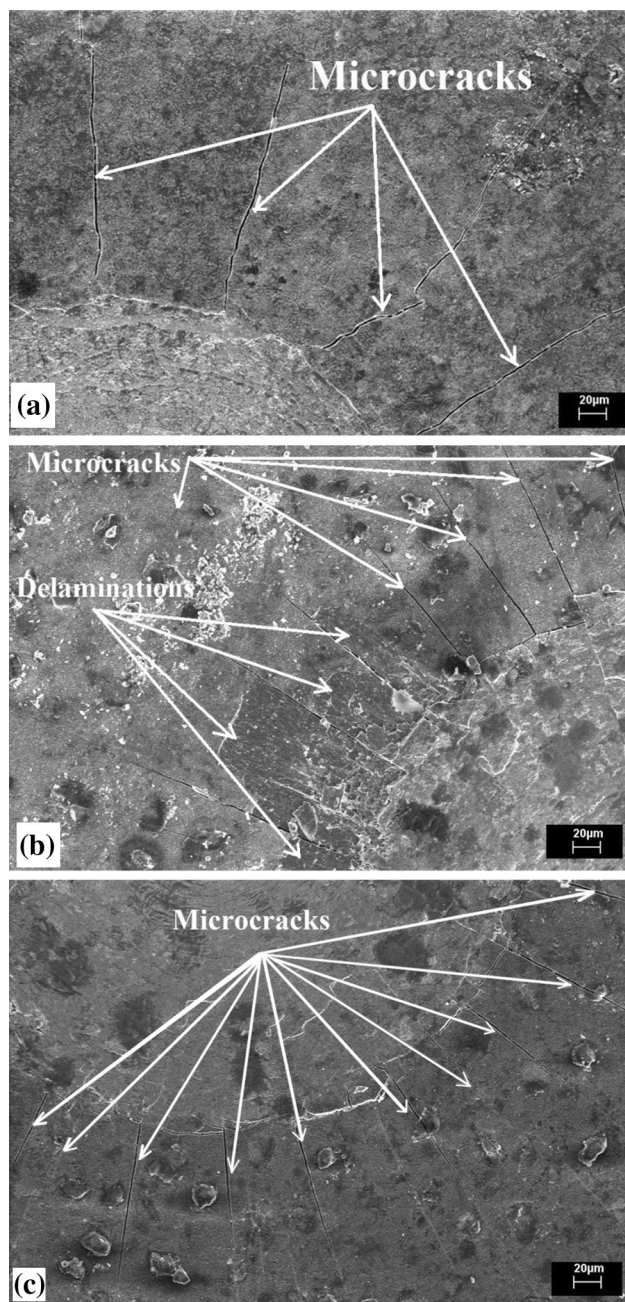


Fig. 5 SEM micrographs of VDI adhesion test of borided **a** AISI P20, **b** AISI H13 and **c** AISI D2 steels at 900 °C for 2 h

range from $2.9 \times 10^{-7} \text{ mm}^3/\text{Nm}$ to $5.5 \times 10^{-7} \text{ mm}^3/\text{Nm}$, those of the borided samples range from $0.06 \times 10^{-7} \text{ mm}^3/\text{Nm}$ to $3.45 \times 10^{-7} \text{ mm}^3/\text{Nm}$. The borided samples show high wear resistance compared to the uncoated samples. The literature survey also reports that boride phases show rather high wear resistance [21, 22].

The lowest wear rate is observed with AISI P20 steel borided at 900 °C for 2 h ($0.06 \times 10^{-7} \text{ mm}^3/\text{Nm}$) while the highest wear rate is seen with AISI H13 borided at

950 °C for 6 h ($3.45 \times 10^{-7} \text{ mm}^3/\text{Nm}$). The Cr content of AISI D2 steel is more than AISI P20 and AISI H13 steels. Therefore, boride layer of AISI D2 steel has thinned and smoothed. This result is compatible with that reported in the literature [23]. The wear behaviors of steels affect parameter such as chemical composition, boriding time and temperature [5, 24, 25].

With an increase in the boriding temperature, boride layer thickness values increases while the wear resistance decreases. X-ray analysis confirms that the FeB, CrB and MnB phases become dominant at high temperatures depending on the chemical composition of steel.

Residual stresses occur in the boride layer and between the boride layer and the base metal after boriding of the metals. The chemical composition of the material, boriding conditions and heat treatments are factors which have an effect on residual stresses. The phase structure of a layer (single-phase or dual-phase) and its geometry (flat or indented) also have an effect on residual stresses [5, 26]. An ideal layer must be of single-phase and its base geometry must have a tooth structure. Residual stresses are due to the difference in the thermal expansion coefficients of FeB ($23 \times 10^{-6} \text{ }^\circ\text{C}^{-1}$) and Fe₂B ($7.85 \times 10^{-6} \text{ }^\circ\text{C}^{-1}$). In dual phase boride layers compressive stress occurs in the Fe₂B phase and tensile stress occurs in the FeB phase after boriding. These stresses cause the layer to crack and the FeB phase to exfoliate [5, 13, 23–27]. When these flakes are stuck between the ball and samples, they increase the wear rate by causing abrasive wear. The wear behaviors of the borided steels used in this study are compatible with the adhesion behaviors. An increase in the boriding temperature and time lead to a decrease in the wear and adhesion features. Optimum boriding temperature and time of AISI P20, AISI H13 and AISI D2 steels are 900 °C and 2 h. Consequently, FeB layer thickness increases due to boriding at high temperature (950 °C) and time (4 and 6 h). The wear rates increases because of poor adhesion properties between FeB and Fe₂B interphases [12].

4 Conclusion

The following conclusions were obtained as a result of the boriding of AISI P20, AISI H13 and AISI D2 steels at 900 and 950 °C temperatures for retention time of 2, 4 and 6 h.

1. Boride types formed on the surface of the borided steels had a smooth morphology. XRD analysis revealed the CrB and the MnB phases in addition to the FeB and Fe₂B phases depending on the chemical composition of the steel.
2. Optical microscope examination after the boriding process revealed that the boride layer had a uniform

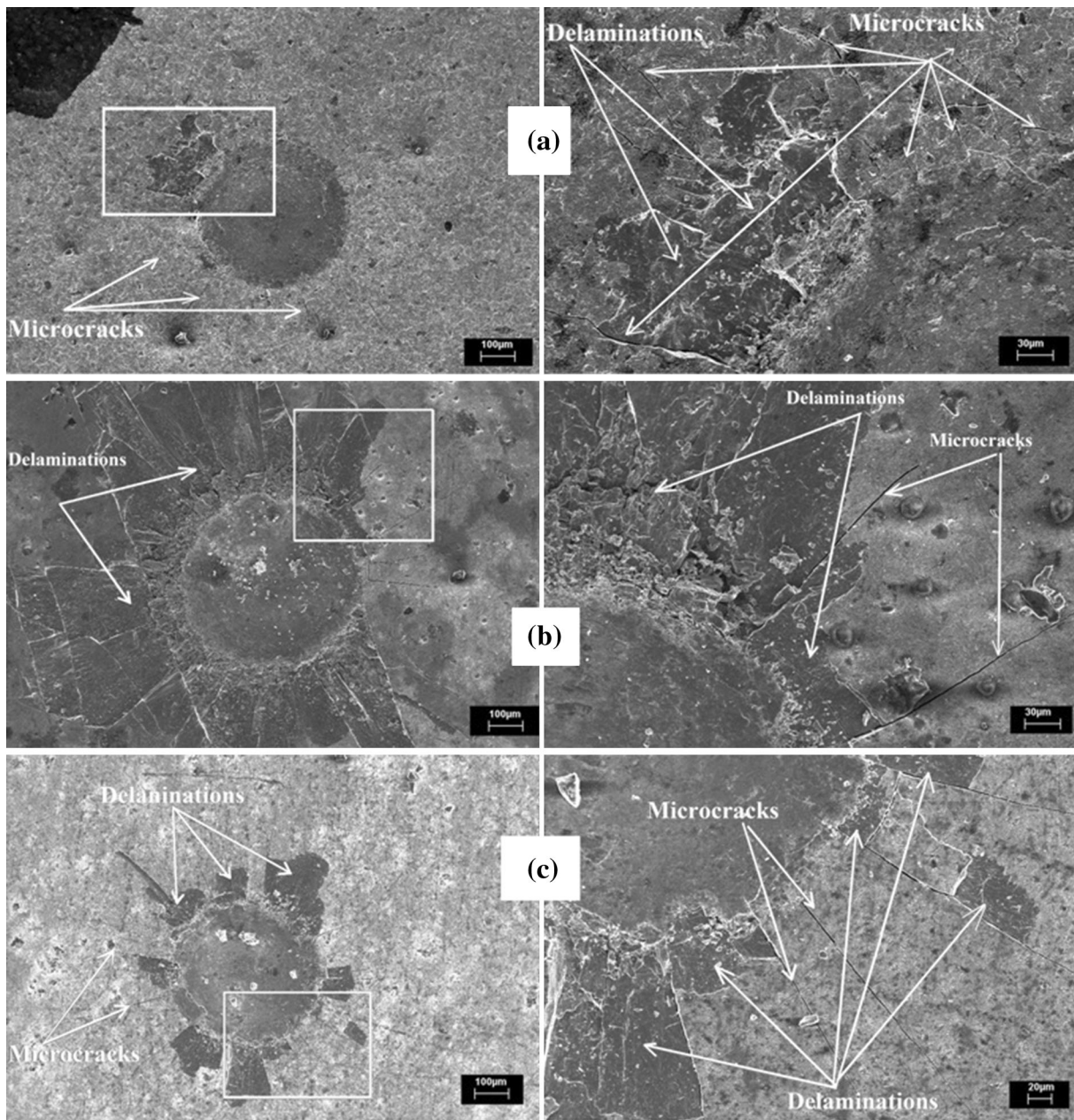


Fig. 6 SEM micrographs of VDI adhesion test of borided **a** AISI P20, **b** AISI H13 and **c** AISI D2 steels at 950 °C for 6 h

Table 3 Adhesion strength quality (HF1–HF6) of AISI P20, H13 and D2 steels borided at 900 and 950 °C

Substrate	Boriding temperature (°C)	
	VDI 3198 Rockwell-C indentation failure map	
	900	950
AISI P20	HF1–HF2	HF1–HF2
AISI H13	HF1–HF2	HF4–HF5
AISI D2	HF2–HF3	HF5

thickness in all the three steels. The boride layer thickness changed depending on the chemical composition of the substrate materials and the boriding time and temperature.

3. The surface hardness values of AISI P20, AISI H13 and AISI D2 steels increased about fourfold–fivefold with the boriding process.
4. The HRC indentation test results indicated that, according to the maps, the adhesion quality of the boride coating was sufficient for all the steels at low

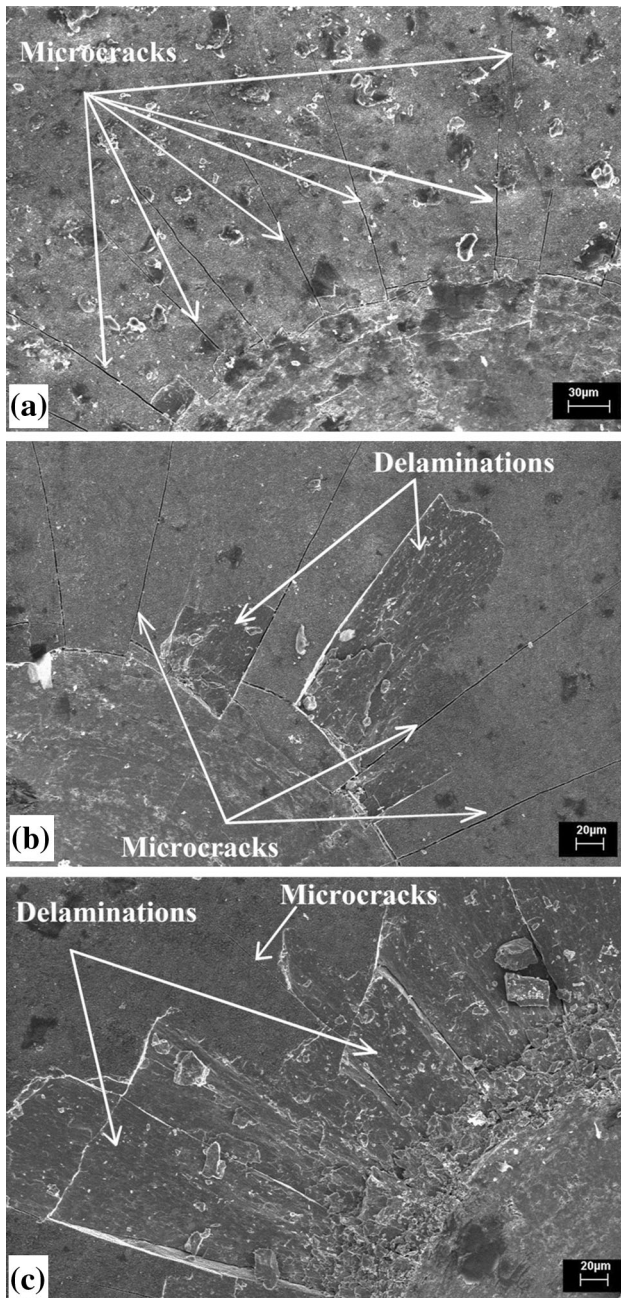


Fig. 7 SEM micrographs of VDI adhesion test on Borided AISI H13 steel **a** boriding at 900 °C for 2 h **b** boriding at 900 °C for 4 h and **c** boriding at 900 °C for 6 h

temperatures and retention times. The adhesion quality of AISI P20 and AISI D2 steels was much better compared to that of AISI H13 steel. In addition, the adhesion capacity decreased with an increase in the boriding time and temperature.

- The best wear resistance was obtained in AISI P20 and AISI D2 steels. The wear resistance and adhesion capacity of the coatings were observed to be directly

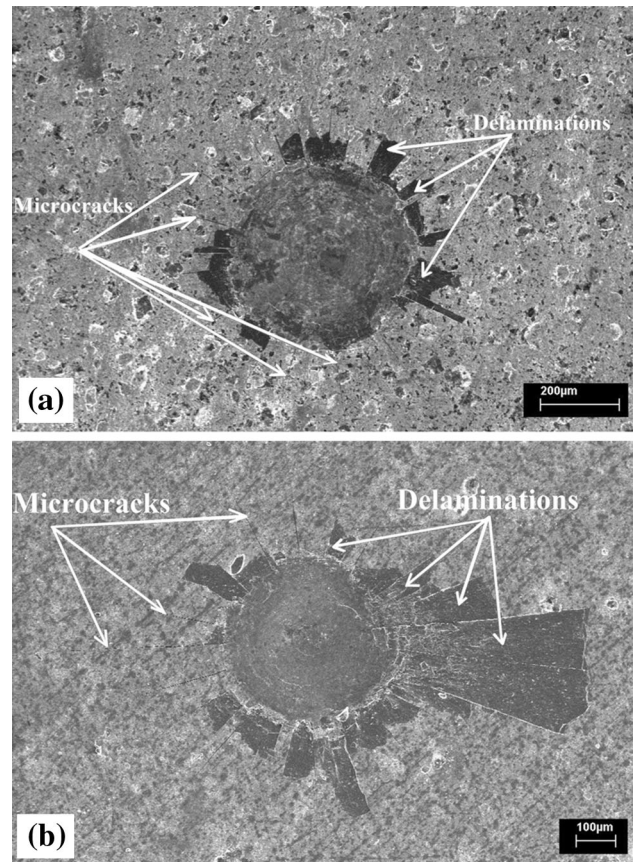


Fig. 8 SEM micrographs of VDI adhesion test on Borided AISI D2 steel **a** boriding at 900 °C for 4 h **b** boriding at 950 °C for 4 h

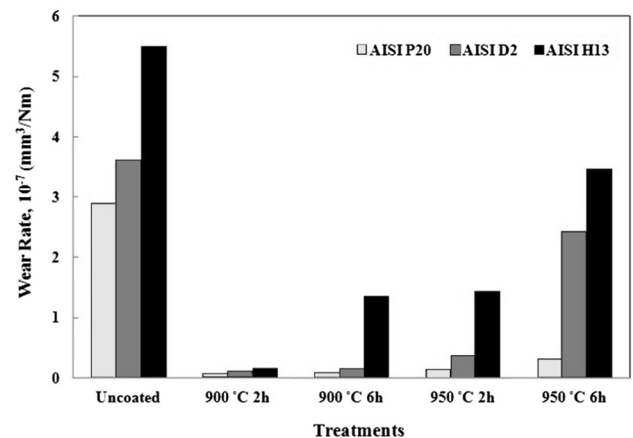


Fig. 9 Variation of wear rates with boronizing time and boriding temperature of borided steels

proportional. The adhesion capacity of the boride layer onto the surfaces of the steels as well as wear resistance decreased with an increase in the boriding time and temperature.

References

1. Maragoudakis N, Stergioudis G, Omar H, Paulidou H, and Tsipas D N *Mater Lett* **57** (2002) 949.
2. Ozbek I, and Bindal C, *Surf Coat Technol* **154** (2002) 14.
3. Ozdemir O, Omar M A, Usta M, Zeytin S, Bindal C, and Ucisik A H, *Vacuum* **83** (2009) 175.
4. Ozbek I, Akbulut H, Zeytin S, Bindal C, and Ucisik A H, *Surf Coat Technol* **126** (2000) 166.
5. Sinha A K, *Heat Treat ASM Handbook* **4** (1997) 437.
6. Taktak S, *Mater Des* **28** (2007) 1836.
7. Uslu I, Comert H, Ipek M, Ozdemir O, and Bindal C, *Mater Des* **28** (2007) 55.
8. Oliveira C K N, Casteletti L C, Lombardi Neto A, Totten G E, and Heck S C, *Vacuum* **84** (2010) 792.
9. Vidakis N, Antoniadis A, and Bilalis N, *J Mater Process Technol* **481** (2003) 143.
10. Verein Deutscher Ingenieure Normen, *VDI 3198* (1991) Dusseldorf, VDI-Verlag.
11. Daimler Benz Adhesion Test, *Verein Deutscher Ingenieure (VDI) Richtlinie 3198* (1992) 7.
12. Kayali Y, and Taktak S, *J Adhes Sci Technol* **29** (2015) 2065.
13. Meric C, Sahin S, and Yilmaz S S, *Mater Res Bull* **35** (2000) 2165.
14. Melendez E, Campos I, Rocha E, et al, *Mater Sci Eng A* **234** (1997) 900.
15. Carbuicchio M, and Palombarini G, *J Mater Sci Lett* **6** (1987) 1147.
16. Genel K, *Vacuum* **80** (2006) 451.
17. Efe G C, Ipek M, Ozbek I, Zeytin S, Bindal C, *Mater Charact* **59** (2008) 23.
18. Kayali Y, *Phys Metals Metallogr* **114** (2013) 1061.
19. Taktak S, and Tasgetiren S, *J Mater Eng Perform* **15** (2006) 570.
20. Kayali Y, Yalcin Y, and Taktak S, *Mater Des* **32** (2011) 4295.
21. Tabur M, Izciler M, Gulb F, and Karacan I, *Wear* **266** (2009) 1106.
22. Celikyurek I, Baksan B, Torun O, and Gurler R, *Intermetallics* **14** (2006) 136.
23. Hunger H J, and Trute G, *Heat Treat* **2** (1994) 31.
24. Tsipas D N, and Rus J, *J Mater Sci Lett* **6** (1987) 118.
25. Kayali Y, *J Balkan Tribol Assoc* **19** (2013) 340.
26. Fichtl W, Trausner N, and Matuschka AG, in *Boronizing with Ekabor*. Elektroschmelzwerk Kempten GmbH, Wolfson Heat Treatment Centre, Univ Aston Birmingham, Gosta Green, Birmingham (1987).
27. Subrahmanyam J, and Gopinath K, *Wear* **95** (1984) 287.